Neuropilin-1, a myeloid cell-specific protein, is an inhibitor of HIV-1 infectivity

Shumei Wang[a,b,1], Li Zhao[a,b,1], Xiaowei Zhang[a,b], Jingjing Zhang[c], Hong Shang[a,b,d], and Guoxin Liang[a,b,c,d,2]

[a]Key Laboratory of AIDS Immunology of Ministry of Health, Department of Laboratory Medicine, The First Affiliated Hospital, China Medical University, Shenyang 110122, China; [b]National Clinical Research Center for Laboratory Medicine, The First Affiliated Hospital, China Medical University, Shenyang 110122, China; [c]Research Institute for Cancer Therapy, The First Affiliated Hospital, China Medical University, Shenyang 110122, China; and [d]Key Laboratory of AIDS Immunology, Chinese Academy of Medical Sciences, Shenyang 110001, China

Edited by Michael Oldstone, Department of Immunology and Microbiology, The Scripps Research Institute, La Jolla, CA; received August 23, 2021; accepted November 23, 2021

Myeloid lineage cells such as macrophages and dendritic cells (DCs), targeted by HIV-1, are important vehicles for virus dissemination through the body as well as viral reservoirs. Compared to activated lymphocytes, myeloid cells are collectively more resistant to HIV-1 infection. Here we report that *NRP-1*, encoding transmembrane protein neuropilin-1, is highly expressed in macrophages and DCs but not CD4$^+$ T cells, serving as an anti-HIV factor to inhibit the infectivity of HIV-1 progeny virions. Silencing *NRP-1* enhanced the transmission of HIV-1 in macrophages and DCs significantly and increased the infectivity of the virions produced by these cells. We further demonstrated that NRP-1 was packaged into the progeny virions to inhibit their ability to attach to target cells, thus reducing the infectivity of the virions. These data indicate that NRP-1 is a newly identified antiviral protein highly produced in both macrophages and DCs that inhibit HIV-1 infectivity; thus, NRP-1 may be a novel therapeutic strategy for the treatment of HIV-1 infection.

HIV-1 | myeloid cells | NRP-1 | macrophage | dendritic cell

HIV-1 primarily targets two groups of cells in vivo, CD4$^+$ T lymphocytes and myeloid lineage cells such as macrophages and dendritic cells (DCs) (1). Monocytes and granulocytes are collectively called myeloid cells, which originate from hematopoietic stem cells in the bone marrow and are continuously supplied to all tissues via the circulation (2–4). Monocytes mature into macrophages in various tissues, such as the Kupffer cells in the liver and alveolar macrophages in the lungs. Monocytes can also differentiate into DCs in lymphoid organs and Langerhans cells in the skin, functioning as professional antigen-presenting cells.

Primary circulating blood monocytes, along with differentiated macrophages and DCs, are critical in the immune responses to HIV-1 infection. Macrophages and DCs are important targets for HIV-1 replication in vivo; they both serve as vehicles for virus dissemination through the body and viral reservoirs (1, 5, 6). While myeloid cells can support the persistent replication of HIV-1, they do not support the high productivity of HIV-1, in contrast to infected T cells. This resistance varies according to the differentiation status of the myeloid cells, the presence or absence of stimulation, and the different steps in the viral life cycle. For example, a major impairment of HIV-1 occurs during the early phases of infection, such as the inhibition of HIV reverse transcription by SAMHD1 in DCs (7, 8). Nevertheless, the blockage of HIV-1 infection in the later infection phase in these cells remains elusive.

In this study, we investigated whether myeloid cells had factors that restricted HIV-1 infection in the late phases. We conducted experiments to identify and compare the cellular protein produced by macrophages and activated CD4$^+$ T lymphocytes that were incorporated into virions. As a result, we uncovered a transmembrane protein, neuropilin-1 (NRP-1) (9–14), that was only present in the virions produced in macrophages but not CD4$^+$ T cells. Here, we report that the gene encoding NRP-1, a newly identified antiviral factor, is highly expressed in macrophages and DCs. Also, NRP-1 is packaged into virions to restrict HIV-1 infectivity by blocking their attachment to target cells. These findings suggest that NRP-1 can be a novel anti-HIV therapeutic target.

Results

NRP-1 Is Found inside Viral Particles Only in Macrophages. We aimed to identify the factors in myeloid lineage cells that inhibited the late phase of HIV-1 infection. Thus, we investigated the cellular factors packaged in the progeny virions produced in primary macrophages and compare them to those produced in stimulated CD4$^+$ T lymphocytes (Fig. 1*A*). We compared the virions produced by primary macrophages to those in CD4$^+$ T cells by infecting monocyte-derived macrophages (MDMs) and CD4$^+$ T cells with dual-trophic HIV-1$_{89.6}$ and allowing HIV to spread among these cells for 10 d. The media obtained from primary MDMs and CD4$^+$ T cells containing the same number of HIV-1 particles were subsequently layered on a 20% sucrose solution for ultracentrifugation. Then, the virion pellets were purified using anti-CD44 microbeads and a magnetic-based method and subsequently analyzed using liquid chromatography and mass spectrometry (MS) to identify the cellular proteins incorporated into the virions. NRP-1, originally identified

Significance

Macrophages and dendritic cells represent an important target for HIV-1 replication in vivo as they serve both as a vehicle for virus dissemination throughout the body and a viral reservoir. However, myeloid cells can support persistent replication of HIV-1 and, in contrast to infected T cells, demonstrate lower productivity. Using proteomics, we discovered that NRP-1 is a host restriction factor that inhibits HIV-1 from infecting macrophages and dendritic cells. NRP-1 is incorporated into the HIV-1 virion particle to inhibit its ability to attach to target cells in a viral envelope glycoprotein-independent manner. Overall, these results provide insights into the ability of myeloid lineage cells to utilize NRP-1 to interfere with HIV-1 infection.

Author contributions: G.L. designed research; S.W., L.Z., X.Z., J.Z., and G.L. performed research; G.L. contributed new reagents/analytic tools; X.Z., J.Z., H.S., and G.L. analyzed data; and G.L. wrote the paper.

The authors declare no competing interest.

This article is a PNAS Direct Submission.

[1]S.W. and L.Z. contributed equally to this work.

[2]To whom correspondence may be addressed. Email: gxliang@cmu.edu.cn.

This article contains supporting information online at http://www.pnas.org/lookup/suppl/doi:10.1073/pnas.2114884119/-/DCSupplemental.

Published January 5, 2022.

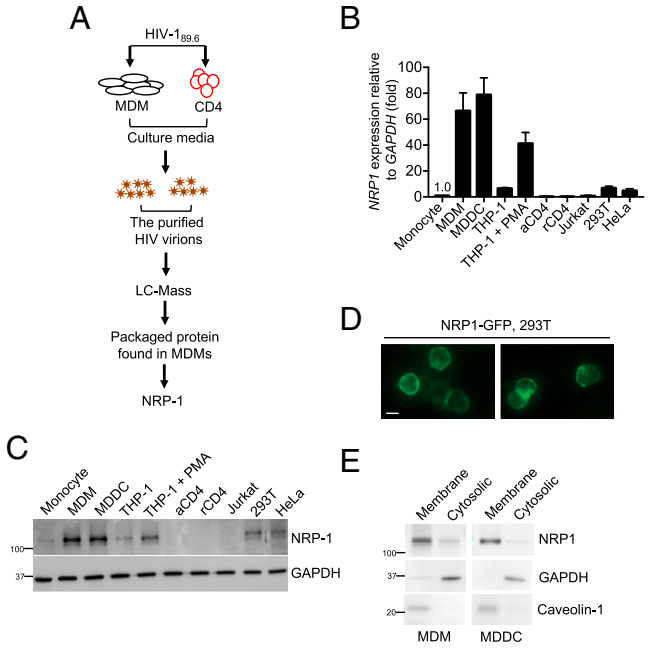

Fig. 1. NRP-1 is incorporated into HIV-1 virion and is mainly expressed in macrophages and DCs. (*A*) The schematic representation of the experimental design used to identify NRP-1 in HIV-1 virions. (*B* and *C*) Total RNA was extracted from primary monocytes, MDMs, MDDCs, THP-1, PMA-treated THP-1, stimulated or resting CD4$^+$ T cells, established cell lines 293T cells, HeLa cells, and Jurkat cells. *NRP-1* transcript levels were measured using qPCR and then normalized to *GAPDH* levels (*B*). Meanwhile, Western blotting was conducted to assess the level of NRP-1 and GAPDH (*C*). (*D*) The 293T cells exogenously expressing the vector encoding NRP-1-GFP were visualized by microscopy. (Scale bar, 10 μm.) (*E*) MDMs or MDDCs were lysed, and membrane-bound and cytosolic proteins were separated to assess the levels of NRP-1, Caveolin-1, and GAPDH using Western blotting with specific antibodies. All blotting data are representative of three independent experiments.

as a neuronal and endothelial cell receptor required for embryonic development, axon guidance, and vasculature formation (15–17), was found in HIV-1 particles produced from macrophages and not from CD4$^+$ T cells (*SI Appendix*, Table S1) (9–14). To validate NRP-1's incorporation into viral particles, we infected primary MDMs with or without HIV-1 (*SI Appendix*, Fig. S1*A*) and lysed the purified virions to prepare them for Western blotting. As a result, NRP-1 was detected inside virion particles by its specific antibody only in the presence of HIV-1 infection (*SI Appendix*, Fig. S1*B*), suggesting that NRP-1 is packaged with HIV-1 virions. We also examined whether overexpressed NRP-1 is packaged into HIV-1 virions and observed that only NRP-1, but not green fluorescent protein (GFP), was detected in the purified virions (*SI Appendix*, Fig. S1*C*). Importantly, both virion-associated envelope (Env) and capsid (CA) proteins were intact in the presence of NRP-1, indicating that NRP-1 did not affect viral progeny assembly and maturation.

NRP-1 is also expressed by several types of immune cells in which it participates in critical immune functions (18). Interestingly, in addition to being induced in infiltrating mouse CD8$^+$ T cells involved in cancer immunotherapy, NRP-1 enhances human T cell leukemia virus type-1 (HTLV-1), murine cytomegalovirus (MCMV), and severe acute respiratory syndrome coronavirus 2 (SARS-CoV-2) infection of target cells (9–12). Therefore, we wanted to examine the expression profile of *NRP-1* in various target cells of HIV-1. *NRP-1* was found to be highly expressed in macrophages, DCs, and PMA-stimulated THP-1 cells and mildly expressed in 293T, HeLa cells; however, its expression is minimal in stimulated or resting CD4$^+$ T cells or Jurkat cells (Fig. 1 *B* and *C*). Since NRP-1 is expressed at a low level in CD4$^+$ T cells, it is not surprising that NRP-1 was not detected inside virions produced from CD4$^+$ T cells.

Moreover, we found that interferon (IFN) treatment did not up-regulate *NRP-1* expression in macrophages or DCs (*SI Appendix*, Fig. S2 *A* and *B*). In addition, except for IFN-γ, IFN-α and IFN-β could not induce *NRP-1* expression in stimulated CD4$^+$ T cells (*SI Appendix*, Fig. S1 *C*–*E*). These results suggest that NRP-1 is not involved in IFN-mediated antiviral activities either in macrophages or DCs. Although IFN-γ slightly up-regulates *NRP-1* expression in stimulated CD4$^+$ T cells, the resultant amount of NRP-1 might be insufficient for involvement in IFN-γ mediated antiviral activities.

NRP-1 is also a transmembrane protein (9–17). Thus, we first analyzed its cellular localization in 293T cells using the fusion protein NRP-1-GFP. NRP-1-GFP was confirmed to emit a clear fluorescent membrane signal in 293T cells (Fig. 1*D*). Afterward, we examined the localization of NRP-1 in primary macrophages or DCs. We observed that NRP-1 was consistently located on the cell membrane in a manner similar to Caveolin-1, which is an integrated plasma membrane protein (Fig. 1*E*). These data suggest that NRP-1 is synthesized in macrophages and DCs and packaged into HIV-1 particles.

NRP-1 Restricts HIV-1 Infectivity. First, we investigated the anti–HIV-1 activity of NRP-1 in target cells. As results, we did not observe any effect of NRP-1 on the HIV-1 infection of target cells (*SI Appendix*, Fig. S3*A*), suggesting that NRP-1 does not inhibit HIV-1 replication in the early phase of replication. Next, we explored the antiviral activity of NRP-1 in producer cells by transfecting HIV-1$_{NL4\text{-}3\text{-}Luc}$ reporter vectors combined with the expression of VSV-G or various HIV-1 CXCR4- or CCR5-tropic Env proteins into 293T cells in the presence or absence of NRP-1. We did not observe that NRP-1 affected HIV-1 production. Nevertheless, when we used the same amount of the produced virion to infect 293T cells that expressed the HIV-1 receptor/coreceptors, CD4, CCR5, and CXCR4, we found that NRP-1 obviously inhibited HIV-1 infectivity (*SI Appendix*, Fig. S3*B*), and the levels of HIV-1 late reverse transcription products (Late RT) were also reduced in the presence of NRP-1 (*SI Appendix*, Fig. S3*C*). These results suggested that NRP1 may restrict HIV-1 entry into target cells.

Next, we examined NRP-1 activity with replication-competent proviral vectors in the producer cells. After we measured the viral progeny production, we consistently found that the *NRP-1* expression vectors at different dosages did not affect the production of different isolates of HIV-1 (NL4-3, BaL, AD8, and 89.6) or simian immunodeficiency virus (SIV) (*SI Appendix*, Fig. S4*A*). On the other hand, the presence of NRP-1 significantly inhibited the infectivity of these HIV-1 isolates in a dose-dependent manner (Fig. 2 *A*, *Upper*), whereas it mildly affected the infectivity of SIV isolates (Fig. 2*B*) when we used the same titers of HIV-1 or SIV to infect TZM-bl reporter cells. The highest dosages of NRP-1 could significantly reduce HIV-1 infectivity, such as that of HIV-1$_{NL4\text{-}3}$ by 261-fold, HIV-1$_{89.6}$ to 143-fold reduction, HIV-1$_{BaL}$ by 583-fold, and HIV-1$_{AD8}$ by 134-fold reduction. In contrast, NRP-1 can reduce SIV infectivity by nearly twofold reduction at the highest dosage. Meanwhile, we also analyzed the level of gp120 in the virions in the same number of HIV-1 particles (Fig. 2 *A*, *Lower*) and found that NRP-1 did not affect the gp120 levels. One possibility is that NRP-1 might be incorporated into HIV-1 particles, thereby inhibiting their infectivity. We also titrated input virions to infect TZM-bl reporter cells in the presence or absence of efavirenz to validate the inhibitory effect of NRP-1 on HIV-1. As results, the infectivity of different input viruses from NRP1-expressing cells

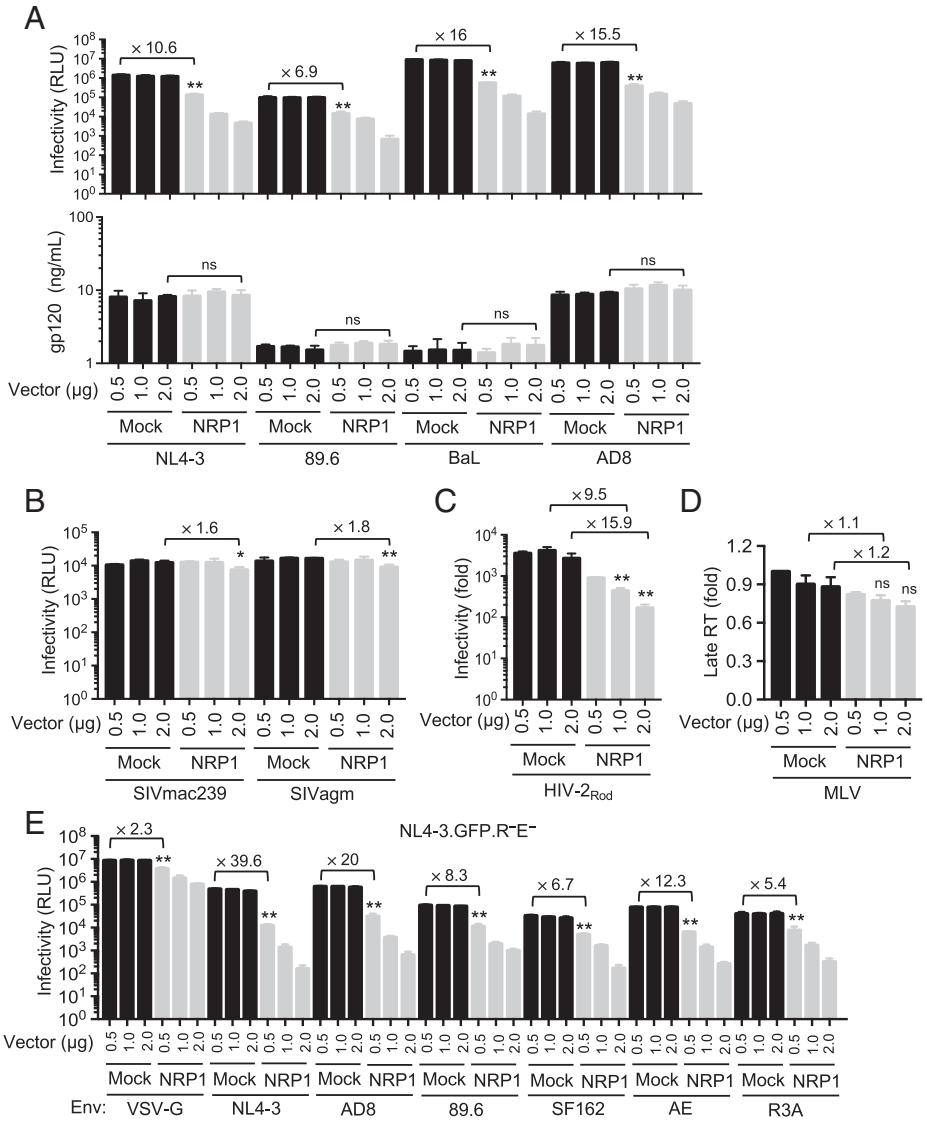

Fig. 2. NRP-1 restricts HIV-1 infectivity. (*A*) The 293T cells were cotransfected with a construct encoding FLAG-tagged NRP-1 or the mock expression construct at different doses, along with HIV-1 proviral vectors. Two days after transfection, 100 ng of the produced HIV-1 virions in the supernatants were used to infect TZM-bl indicator cells to measure viral infectivity (*Upper*) and the level of gp120 using ELISA (*Lower*). $^{**}P < 0.01$; ns, not significant. (*B*–*D*) The 293T cells were cotransfected with the construct encoding FLAG-tagged NRP-1 or the mock expression construct at different doses, along with SIV (*B*), HIV-2 (*C*), and MLV (*D*) proviral vectors. Two days after transfection, the same titers of HIV-2 or SIV were used to infect TZM-bl reporter cells to measure viral infectivity. Mouse NIH 3T3 cells were infected with the same titers of MLV, and their late reverse-transcript products were measured by qPCR. $^{**}P < 0.01$; $^{*}P < 0.05$; ns, not significant. (*E*) The 293T cells were cotransfected with the construct encoding FLAG-tagged NRP-1 or a mock expression construct at different doses, along with a pNL4-3.GFP.R$^-$E$^-$ reporter vector combined with various expression constructs of HIV-1 X4-, R5-trophic, or dual-trophic Env or VSV-G as indicated. Two days after transfection, 100 ng of the produced HIV-1 virions in the supernatants were used to infect the TZM-bl cells to measure viral infectivity. $^{**}P < 0.01$; $^{*}P < 0.05$.

was consistently reduced compared to that of the control viruses (*SI Appendix*, Fig. S4 *B* and *C*).

Interestingly, there are two forms of neuropilins, NRP-1 and NRP-2 (see Fig. 4*A*), and their respective genes exhibit distinct expression patterns. However, NRP-1 and NRP-2 share a common domain organization with and 44% amino acid sequence identity in humans (19). They are composed of five extracellular structural domains—a1 at the N terminus, followed by a2, b1, b2, c, and a single transmembrane helix and a short cytoplasmic tail (20–24). Domains a1 and a2 belong to the structural family of CUB domains, while domains b1 and b2 share structural homology to coagulation factor V/VIII domains (21, 22, 24, 25). Therefore, we also investigated the effect of NRP-2 on HIV-1 infectivity. We did not observe any effect of NRP-2 on the infectivity of HIV-1_{NL4-3} despite NRP-2's sharing 44% amino acid identity with NRP-1 (*SI Appendix*, Fig. S4*D*). These results suggest NRP-1 is the only member of its family with anti–HIV-1 activity.

Moreover, we explored the inhibitory effect of NRP-1 on viruses by overexpressing NRP-1 with HIV-2 (Fig. 2*C*) and murine leukemia virus (MLV) (Fig. 2*D*) replication-competent proviral vectors in producer cells. NRP-1 also displayed a strong inhibitory effect on HIV-2_{Rod} infectivity but not on MLV infectivity. Thus, NRP-1 appears to have preferential inhibitory effect on HIV and SIV but not on MLV. In addition, we observed that NRP-1 could consistently cause a substantial reduction in HIV-1 infectivity when we used the same titers of reporter HIV-$1_{NL4-3.GFP.R-E-}$ with the expression of the VSV-G

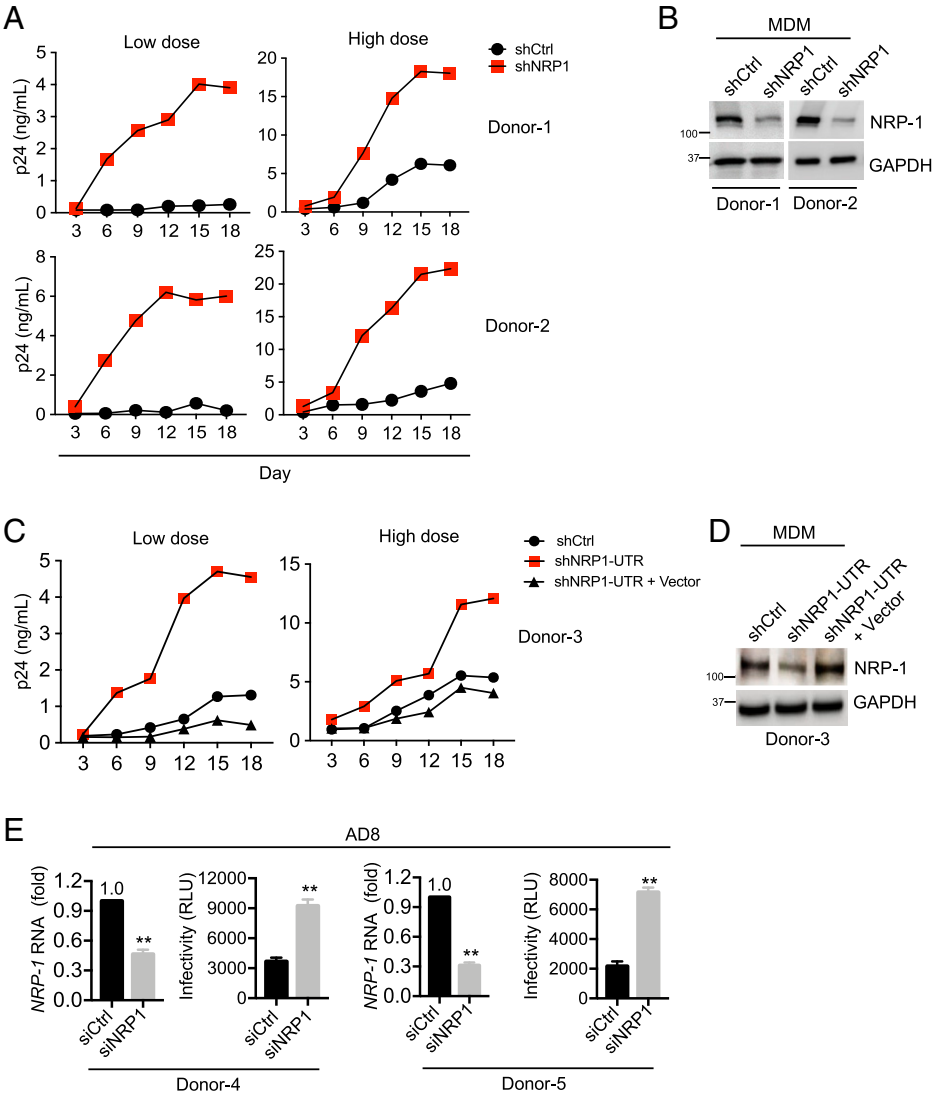

Fig. 3. NRP-1 inhibits HIV-1 infection in macrophages. (*A* and *B*) Lentiviral shRNA-transduced MDMs were infected with 10 (low-dose) or 100 (high-dose) ng of HIV-1_{AD8} for 18 d. Viral production was measured using p24 ELISA at the indicated time points (*A*). The aliquoted cells were lysed for Western blotting to assess the levels of NRP-1 and GAPDH (*B*). (*C* and *D*) MDMs were transduced with lentiviral shRNA targeting the 3′-UTR of the *NRP-1* or control transcript, and the *shNRP-1*-depleted MDMs were then transduced with or without a lentiviral expression vector encoding an untagged NRP-1. Next, the MDMs were infected with 10 (low-dose) or 100 (high-dose) ng HIV-1_{AD8} for 18 d, and viral production was measured by p24 ELISA at the indicated time points (*C*). The shRNA-transduced MDMs were lysed for Western blotting to assess the levels of NRP-1 and GAPDH (*D*). (*E*) The MDMs transfected with siRNA targeting *NRP-1* or the control were infected with HIV-1_{AD8} (multiplicity of infection = 1) and washed twice with PBS to remove the input viruses 6 h after infection. At 3 d after infection, 20 ng of the produced HIV-1 virions in the supernatants were used to infect TZM-bl indicator cells to measure viral progeny infectivity. Total RNA was extracted from the MDMs for qPCR to measure *NRP-1* transcript levels normalized to *GAPDH* levels. $^{**}P < 0.01$.

gene or various HIV-1 CXCR4-, CCR5-, or dual-tropic *Env* to infect TZM-bl cells (Fig. 2*E*). In contrast to HIV-1 Env, when combined with VSV-G, NRP-1 exhibited a mild inhibitory effect on infectivity. Overall, NRP-1 is likely a novel anti–HIV-1 factor of HIV particle infectivity.

NRP-1 Restricts HIV-1 Spread in Macrophages and DCs. We next investigated the anti-HIV activity of NRP-1 in macrophages because *NRP-1* is highly expressed in myeloid lineage cells such as primary macrophages, DCs, and stimulated THP-1 cells. First, we transduced lentiviral short hairpin RNA (shRNA) vectors into THP-1 cells to deplete endogenous NRP-1 and then transfected NL4-3 proviral vectors into these THP-1 cells. Afterward, we used the same numbers of the produced virions from these THP-1 cells to infect TZM-bl reporter cells. NRP-1 depletion increased HIV-1 progeny infectivity in THP-1 cells by nearly eightfold (*SI Appendix*, Fig. S5 *A* and *B*), suggesting that endogenous NRP-1 could act against HIV-1 infectivity in myeloid cells.

Then, we transduced shRNA lentiviral vectors targeting *NRP-1* into primary MDMs and further infected these cells with different dosages of replication-competent HIV-1_{AD8} for 18 d (Fig. 3 *A* and *B*). The silencing of *NRP-1* could noticeably enhance the spread of HIV-1 during the 18-d infection of the macrophages. Moreover, when we applied a lentiviral shRNA targeting the 3′ untranslated region (3′-UTR) of the *NRP-1* transcript, the inhibition of HIV-1 spread was rescued in the endogenous NRP-1–depleted primary MDMs transduced with an exogenous *NRP-1* expression lentiviral vector during HIV-1 infection of macrophages (Fig. 3 *C* and *D*). The exogenous *NRP-1* expression was not affected by this shRNA because it did not affect the expression of *NRP-1* derived from its

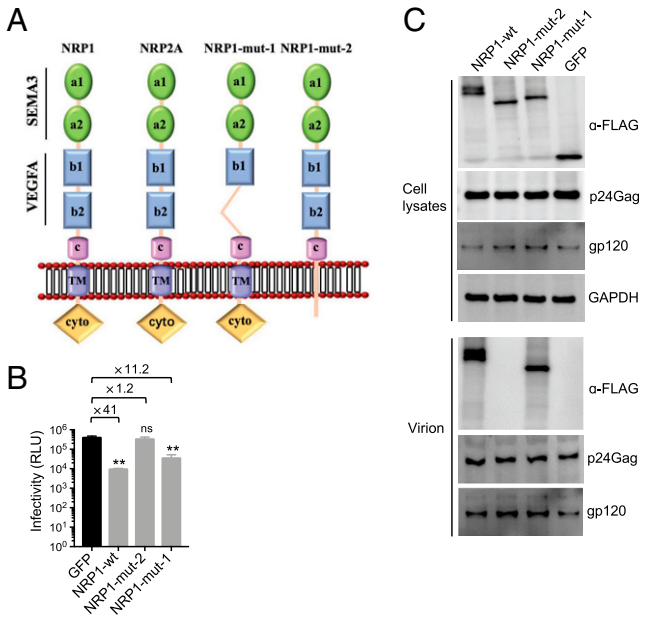

Fig. 4. NRP-1 is incorporated into virions to restrict HIV-1 infection. (*A*) The schematic representation of NRP-1 domains. The full-length NRP-1 possesses a ligand-binding ectodomain consisting of a1/a2 and b1/b2 domains, followed by a membrane-proximal c domain involved in oligomerization. The remainder of the protein comprises a short membrane-spanning region and cytoplasmic tail (cyto). (*B* and *C*) NRP-1 is incorporated into viral particles to inhibit infectivity. The 293T cells were cotransfected with constructs encoding FLAG-tagged NRP-1 or its mutants and GFP, along with NL4-3 proviral vectors. At 2 d after cotransfection, 100 ng of the produced HIV-1 virions in the supernatants were used to infect TZM-bl indicator cells to measure viral progeny infectivity (*B*), and the cells were lysed for Western blotting to assess the levels of NRP-1, its mutants, Gag, gp120, and GAPDH with their specific antibodies. The produced virion particles in the cell supernatants were enriched by sucrose cushion ultracentrifugation and subsequently isolated using anti-CD44 microbeads with a magnetic-based method. The purified virion was lysed for Western blotting to assess the NRP-1 or its mutants, CA (p24), and gp120 levels (*C*). All blotting data are representative of three independent experiments. $^{**}P < 0.01$; ns, not significant.

expression vector, into which the *NRP-1* open reading frame was cloned.

We then validated these results from the shRNA-mediated knockdown of NRP-1 by employing the small interfering RNA (siRNA)-mediated knockdown of *NRP-1* in primary macrophages. The depletion of NRP-1 using siRNA consistently increased HIV-1_{AD8} infectivity (Fig. 3*E*), suggesting that NRP restricted HIV-1 infection in macrophages. In addition, we noticed that the cell membrane protein Serinc5, a Nef-counteracted host restriction factor, was encapsidated into the Nef-defective HIV-1 virions to inhibit their infectivity. Although endogenous NRP-1 displayed an inhibitory effect on the transmission of wild-type HIV-1 in macrophages, it remained unclear whether Nef could compromise the NRP-1–mediated suppression of HIV-1 infectivity to some extent. Thus, we employed RNA interference (RNAi) to deplete NRP-1 or Serinc5 in the primary MDMs (*SI Appendix*, Fig. S6*A*) transfected with wild-type or Nef-defective HIV-1 proviral vectors. The depletion of NRP-1 similarly increased the infectivity of the wild-type and Nef-defective virions, whereas depletion of Serinc5 enhanced the infectivity of the Nef-defective but not the wild-type virions (*SI Appendix*, Fig. S6*B*). Therefore, the presence of Nef compromises the antiviral activity of Serinc5 but not NRP-1 in macrophages.

Afterward, we also investigated the anti-HIV activity of NRP-1 in monocyte-derived dendritic cells (MDDCs). We treated shRNA-transduced MDDCs with VLP-Vpx to enhance HIV-1 infection and further infected these primary cells with HIV-1_{AD8}. The silencing of *NRP-1* also increased the spread of HIV-1 in the MDDCs from two independent healthy donors for 18 d (*SI Appendix*, Fig. S7 *A* and *B*). These data indicate that NRP-1 is an inhibitor of the late phase of HIV-1 infection both in macrophages and DCs.

NRP-1 Is Incorporated into Virion to Block Its Attachment to Target Cells. Since we observed that NRP-1 was incorporated into HIV-1 particles, we hypothesized that the antiviral activity of NRP-1 could be attributed to its effect on virions. We generated NRP-1 mutants (Δ450–550 and Δ810–923) (Fig. 4*A*) according to recent findings (19, 26) and transfected the expression vectors encoding the wild-type or mutant NRP-1 into 293T cells. The absence of the C terminus (Δ810–923, mut-2) but not that of b2 domain (Δ450–550, mut-1) abolished the inhibitory effects of NRP-1 on HIV-1 infectivity (Fig. 4*B*), suggesting that domain b2 was not important in the antiviral activity of NRP-1. We then examined the NRP-1 mutants' ability to incorporate into virion particles and found that NRP-1-mut-2 without the transmembrane domain was not packaged into viral particles (Fig. 4*C*). In contrast, NRP-1-mut-1 exhibiting inhibitory effect on HIV-1 infectivity was incorporated into viral particles. Therefore, the antiviral activity of NRP-1 relies on its incorporation into virion particles.

Furthermore, we analyzed the entry efficiency of HIV-1 particles into target cells in the presence of NRP-1 using a β-lactamase (BlaM)-fused Vpr entry assay. By this system, we can examine the entry of the virions carrying the BlaM-Vpr fusion protein by measuring the activity of the BlaM delivered to target cells. The HIV-$1_{NL4\text{-}3\text{-}Luc\text{-}R+E-}$ viruses (VSV-G) carrying the BlaM-Vpr reporter protein were produced in 293T cells in the presence or absence of NRP-1; then, these viruses were used to infect primary stimulated $CD4^+$ T cells. The entry efficiency of VSV-G–pseudotyped HIV-1 prepared from *NRP-1*–overexpressing cells was markedly reduced compared to that of the control viruses (Fig. 5*A*), and this result was also observed in five independent experiments (Fig. 5*B*). These data indicated that NRP-1–incorporated HIV-1 particles were severely impaired in their ability to enter target cells and that NRP-1 inhibited HIV-1 virions entry.

Next, we performed HIV-1 virion attachment assays and observed that the ability of the wild-type virion HIV-$1_{NL4\text{-}3}$ to attach to target cells, such as TZM-bl or stimulated $CD4^+$ T cells (Fig. 5*C*), was consistently impaired in the presence of NRP-1 in the produced cells. In addition, HIV-$1_{NL4\text{-}3.GFP.R-E-}$ reporter virus combined with the expression of VSV-G or various HIV-1 CXCR4-, CCR5-, or dual-tropic Env from *NRP-1*–expressing cells were also significantly impaired in their ability to attach to susceptible target cells (*SI Appendix*, Fig. S8). Moreover, the NRP-1 C terminus mutant (Δ810–923, mut-2), which is not incorporated into HIV-1 particles, could not inhibit virion attachment to target cells (*SI Appendix*, Fig. S9 *A* and *B*). However, the NRP-1 mutant (Δ450–550, mut-1), which is incorporated into virions, retained the inhibitory effect on virion attachment to target cells, thereby suggesting that the presence of NRP-1 in virus particles hinders virion interaction with target cells. Furthermore, we employed RNAi to silence *NRP-1* in primary macrophages (Fig. 5 *D* and *E*) or MDDCs (Fig. 5 *F* and *G*) to test whether the NRP-1 of these cells could impair HIV-1 attachment to target cells. The loss of endogenous NRP-1 in MDMs or MDDCs consistently increased the attachment of HIV-1 particles to the target cells. These data demonstrate that NRP-1 is incorporated into virions to inhibit their ability to attach to target cells, thereby reducing the infectivity of the progeny virions.

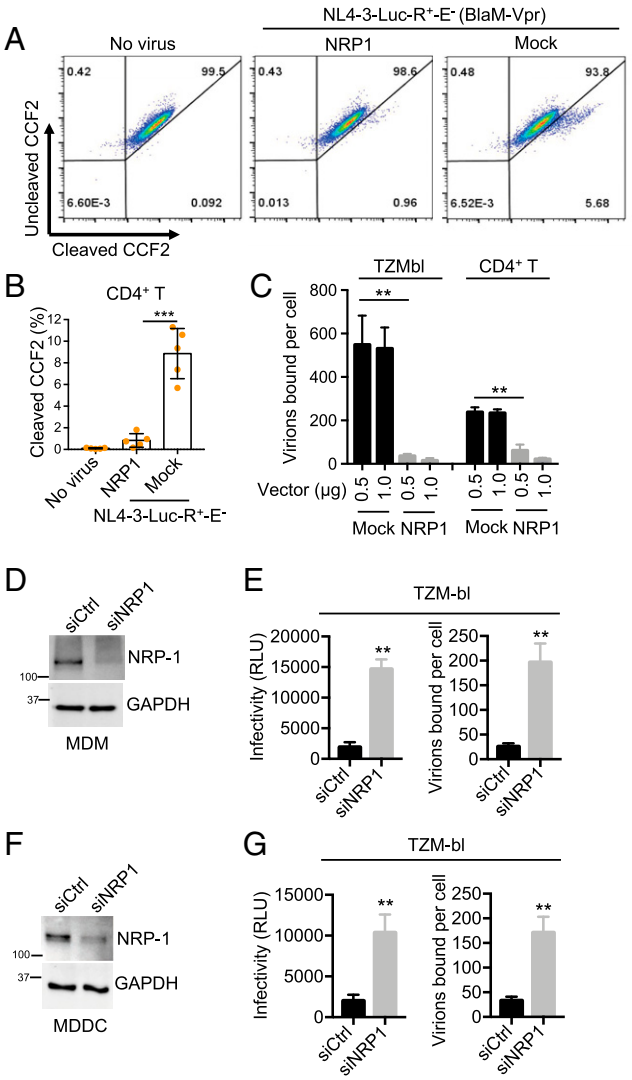

Fig. 5. NRP-1 inhibits HIV-1 virion attachment to target cells. (*A* and *B*) The BlaM-Vpr–based viral entry assay using a VSV-G–pseudotyped HIV-1. The 293T cells were cotransfected with a construct encoding FLAG-tagged NRP-1 or a mock expression construct with or without pNL4-3.GFP.R$^+$E$^-$ reporter vectors (VSV-G) combined with an expression construct encoding BlaM-Vpr. Two days after transfection, 50 ng of the produced virions in the supernatants were used to infect stimulated CD4$^+$ T cells. The fluorescence-activated cell sorter dot plots are representative of five independent experiments (*A*). The data of five independent experiments are plotted as mean ± SEM (*B*). ***$P < 0.001$. (*C*) The HIV-1 attachment assay. The 293T cells were cotransfected with a construct encoding FLAG-tagged NRP-1 or a mock expression construct at different doses, along with HIV-$1_{NL4\text{-}3}$ proviral vectors. Two days after transfection, TZM-bl reporter cells or stimulated CD4$^+$ T target cells were spinoculated with 500 ng of the produced HIV-1 particles at 25 °C for 2 h and washed with PBS twice to remove the input virus after spinoculation. The cells were further lysed for the p24 ELISA to quantify the bound viral particles. (*D*–*G*) MDMs (*D* and *E*) or MDDCs (*F* and *G*) were cotransfected with siRNA targeting *NRP-1* or the control along with HIV-1_{AD8} proviral vectors. At 3 d after cotransfection, the cells were lysed for Western blotting to assess the levels of NRP-1 and GAPDH, and 20 ng of the produced virions in the supernatants were used to infect TZM-bl reporter cells to measure virion infectivity. For HIV-1 attachment assays, TZM-bl cells were spinoculated with 500 ng of the produced virions, and the cells were lysed for p24 ELISAs to quantify the bound viral particles. **$P < 0.01$. All blotting data are representative of three independent experiments.

Discussion

In this study, we have demonstrated that neuropilin family member NRP-1, but not NRP-2, can inhibit the infectivity of HIV-1 progeny virions in macrophages and DCs. *NRP-1* is highly expressed in myeloid lineage cells, such as macrophages and DCs, but not in stimulated or resting CD4$^+$ T lymphocytes. Moreover, *NRP-1* is not induced in IFN-stimulated macrophages, DCs, or CD4$^+$ T cells, suggesting that NRP-1 is not a downstream molecule of IFN against virus infections in host cells. NRP-1 is a transmembrane protein that regulates pleiotropic biological processes, including axon guidance, angiogenesis, and vascular permeability (15–17). It is also a host factor enhancing HTLV, MCMV, and SARS-CoV-2 infection (9–12). However, NRP-1 cannot enhance HIV-1 infection of target cells. In contrast, *NRP-1* expression is strongly inhibitory to the infectivity of various wild-type HIV-1 strains, including NL4-3, 89.6, BaL, and AD8, whereas NRP-1 does not affect HIV-1 production in producer cells. In addition to restricting HIV-1 virion infectivity, *NRP-1* expression in the virus-producer cells can also interfere with the infectivity of HIV-2 and mildly interfere with the infectivity of SIV, whereas it does not affect MLV. The mild inhibitory effect of NRP-1 on SIV infectivity is probably due to insufficient incorporation of NRP-1 into viral particles or the poorly organized structure of packaged NRP-1 in SIV particles. This hypothesis requires further investigation in the future.

Furthermore, we have demonstrated that while NRP-1 is present in intact virion particles, it has no effect on the virion-associated CA and Env proteins. We investigated the molecular mechanisms underlying the antiviral activity of NRP-1 with mutagenesis assays and found that NRP-1 was required to be packaged into viral particles to inhibit their infectivity. Moreover, we demonstrated that NRP-1 inhibited HIV-1 infectivity by interfering with virion attachment to the target cells using virion attachment assays. These data indicate that NRP-1 on the virion surface may sterically disrupt the binding of virions to target cells. In addition, NRP-1 has a highly extended structure with a heavily glycosylated extracellular domain, and its intrinsic structural features may reduce nonspecific binding between the virions and target cells.

Notably, silencing *NRP-1* can promote the transmission of HIV-1 infection in primary macrophages or DCs. On the other hand, ectopic expression of *NRP-1* in endogenously NRP-1–deficient macrophages can rescue the inhibition of HIV-1 transmission. Therefore, we propose that NRP-1 is a macrophage and DC-specific factor located on the cell membrane to inhibit HIV-1 infectivity. Given the critical role of NRP-1 in hindering virion binding to target cells, we also tested whether Nef could compromise the restriction of HIV-1 infectivity by NRP-1. However, we observed that the silencing of *NRP-1* did not preferentially increase the infectivity of Nef-defective HIV-1 compared with wild-type HIV-1 in macrophages. In contrast, silencing *Serinc5* increases the infectivity of Nef-defective but not Nef-positive HIV-1, indicating that Nef counteracts the restriction of Serinc5 to promote HIV-1 infection in primary macrophages. Particularly, NRP-1 also displays an inhibitory effect on the transmission of HIV-1 in DCs.

Myeloid cells generally resist HIV-1 infection compared to CD4$^+$ T cells, probably due to the different genes encoding anti–HIV-1 factors in myeloid cells. Thus, the expression of *NRP-1* in myeloid lineage cells can partially contribute to their resistance to the spread of HIV-1. Since cell–cell transmission of HIV-1 is a major in vivo event, it is necessary to investigate whether NRP-1 restricts the direct transmission of HIV-1 from macrophages or DCs to CD4$^+$ T cells in future research. Notably, NRP-1 is reported to be required within endothelial cells for angiogenesis via vascular endothelial growth factor (VEGF)

signaling (17). Cardiovascular prevention is required in more than half of HIV-1 infected patients because they are prone to developing increased angiogenesis (27). Whether NRP-1 promotes angiogenesis during HIV-1 infection also requires further investigation in the future. Overall, our study provides insights into the ability of myeloid lineage cells to utilize NRP-1 to interfere with HIV-1 infection. Further elucidation of NRP-1's interaction with HIV-1, HIV-2, and other viruses may help develop therapeutic strategies that target viral infections.

Methods

Ethics Statement. This study is approved by the Research and Ethics Committee of The First Affiliated Hospital of China Medical University. All the blood samples were obtained from the healthy donors following the National Health and Medical Research Council guidelines. In addition, informed consent was obtained from each healthy donor before the study. Moreover, the study protocol and informed consent forms were approved by the Institutional Review Board approved of China Medical University.

Cells and Cell Culture Reagents. NIH 3T3 (mouse), 293T (human), and TZM-bl cells were cultured in Dulbecco's modified Eagle's medium (Gibco). THP-1 and Jurkat (human) cells were cultured in RPMI-1640 medium (Gibco). Both media were supplemented with 10% fetal bovine serum (FBS; Gibco), 100 U/mL penicillin, and 100 mg/mL streptomycin. Plasmids were transfected into the 293T cells using Lipofectamine 2000 (Invitrogen).

Peripheral blood mononuclear cells (PBMCs) obtained from healthy blood donors were purified via Ficoll-Hypaque density gradient centrifugation. $CD4^+$ T cells or monocytes were isolated from the PBMCs via negative selection with human $CD4^+$ T cells or a CD14-positive enrichment mixture (STEMCELL Technologies). The $CD4^+$ T cells were stimulated by adding CD3/CD28 activator magnetic beads (Invitrogen) to the culture medium for 2 d with 50 U/mL interleukin (IL)-2 (Biomol). The isolation and culturing of monocytes, MDMs, and MDDCs were performed (28, 29). MDMs were generated by stimulating monocytes with 10 ng/mL recombinant human granulocyte-macrophage colony-stimulating factor (GM-CSF; R&D) and 50 ng/mL recombinant human macrophage colony-stimulating factor (M-CSF; R&D) for 7 d. MDDCs were generated by incubating CD14-purified monocytes in IMDM medium (Gibco) supplemented with 10% FBS, 2 mM L-glutamine, 100 IU/mL penicillin, 100 mg/mL streptomycin, 10 mM Hepes, 1% nonessential amino acids, 1 mM sodium pyruvate, 10 ng/mL GM-CSF, and 50 ng/mL IL-4 (Miltenyi Biotec). On day 4, two-thirds of the culture medium was replaced with a fresh medium containing GM-CSF and IL-4. Immature MDDCs were harvested and used for experiments on day 6. Lipofectamine 3000 (Thermo Fisher) was used to deliver siRNA into MDMs or MDDCs.

Plasmids. The open reading frames of the expression vectors encoding NRP-1 (OriGene) were cloned de novo into pCMV-3Tag-2A (Addgene). Also, HIV-1 reporter vectors of NL4-3.Luc.R-E-, NL4-3.GFP.R^-E^-, and NL4-3.GFP.R^+E^- and proviral vectors of NL4-3-R^-E^-, NL4-3, 89.6, SIV_{mac239}, SIV_{agm}, HIV-2_{Rod}, and MLV (NIH AIDS Program) were obtained. In addition, the proviral vector of HIV-1_{BaL} was gifted by N. R. Landau, New York University, New York City (30), HIV-1_{AD8} was gifted by E. Freed, National Institutes of Health, Frederick, MD, and the MLV-luc reporter vector was gifted by G. Gao, Chinese Academy of Sciences Key Laboratory of Infection and Immunity, Beijing, China.

RNAi in THP-1 Cells, MDMs, or MDDCs. The shRNA-mediated silencing of *NRP-1* (RHS4430-200289197 or RHS4430-200215106 targeting open reading frame; RHS4430-200222352 targeting 3′-UTR) or control (catalog no. RHS4346) was achieved by introducing a microRNA-adapted shRNA lentivirus into the THP-1 cells, MDMs, and MDDCs (28, 29). In summary, the freshly isolated monocytes were treated with Vpx and transduced with an shRNA lentivirus. After puromycin selection, the cells were infected with a replication-competent CCR5-trophic HIV-1 for 6 h and washed twice with cold phosphate-buffered saline (PBS) to remove the input virus. The human ON-TARGET siRNA pools against *NRP-1* [human siRNA-SMARTpool-(L-019484-00-0010)], including 5′-CGAUAAAUGUGGCGAUACU-3′, 5′-GGACAGAGACUGCAAGUAU-3′, 5′-GUAUACGGUUGCAAGAUAA-3′, and 5′-AAGACUGGAUCACCAUAAA-3′ and controls (Nontargeting, D-001810-10-20), including 5′-UGGUUUACAUGUCGACUAA-3′, 5′-UGGUUUACAUGUUGUGUGA-3′, 5′-UGGUUUACAUGUUUUCUGA-3′, and 5′-UGGUUUACAUGUUUUCCUA-3′ (Dharmacon) were purchased. siRNA-mediated silencing was achieved by directly transfecting differentiated THP-1 cells, MDMs, and MDDCs with siRNA using Lipofeztamine 3000 (Thermo Fisher).

Measurement of Viral Infectivity. The levels of p24, p27, or gp120 in culture supernatants were measured using enzyme-linked immunosorbent assay (ELISA) (ABL Corporation). The infectivity of HIV-1, HIV-2, and SIV produced in culture supernatants was measured by infecting TZM-bl reporter cells with the viruses. Then, virus infectivity was quantified using luciferase as a reporter. The luciferase activity in a cell lysate is quantified in relative luminescence units (Promega). Also, the background luminescence of the control (uninfected) TZM-bl cells was subtracted from each data point.

Reverse Transcriptase Assay. HIV-2 or MLV particles were purified, and the level of virion-associated reverse transcriptase was measured using the Reverse Transcriptase (RT) Assay (colorimetric; Roche).

Measurement of Late RT Products of MLV. Mouse NIH 3T3 cells were infected with MLV for 24 h, and genomic DNA was extracted from the cells to quantify late reverse-transcript product using qPCR with specific primers for MLV 5′-CGTCAGCGGGGGTCTTTC-3′ and 5′-CTGGGCAGGGGTCTCCCG-3′ (29, 31).

Quantification of Late RT Products of HIV-1. HIV-1 producer 293T cells were washed twice with PBS to remove the transfected HIV-1 plasmid before infection. The obtained viral stocks were treated for 1 h at 37 °C with DNase I (Takara). DNA was extracted using a DNeasy Blood & Tissue Kit (Qiagen). qPCR was performed to quantify late viral RT with the following primers, as described previously (32): late RT forward: 5′-AGCAGGAACTACTAGTACCC-3′′ and late RT reverse: 5′- TTGTCTTATGTCCAGAATGC-3′′.

Identification of NRP-1 Incorporated into HIV-1 Virions from Macrophages. MDMs generated from the monocytes isolated from five healthy donors were pretreated with VLP-Vpx and infected with 89.6. At 6 h after infection, the cells were washed with PBS twice to remove the input virions and cultivated for 8 d. Meanwhile, $CD4^+$ T cells isolated from the same healthy donors were stimulated and infected with 89.6. At 6 h after infection, the cells were washed with PBS twice and cultivated for 8 d. The cell culture media containing HIV-1 particles were centrifuged for 5 min at 1,200 × *g*. The supernatants were passed through a 0.45-μm filter (Thermo Fisher) and layered on 20% sucrose for a 2-h ultracentrifugation at 25,000 × *g* at 4 °C. The obtained virion pellets were resuspended in 200 μL of PBS with 50 μL of anti-CD44 microbeads for 30 min at room temperature, and the viable and infectious HIV-1 particles were further isolated by a magnetic-based method according to the manufacturer's instructions (μMACS VitalVirus HIV Isolation Kit; Miltenyi Biotec). The isolated HIV-1 virions were subsequently reduced in 20 mM dithiothreitol (Sigma) at 95 °C for 5 min and alkylated in 50 mM iodoacetamide (Sigma) for 30 min in the dark at room temperature. After alkylation, the samples were transferred to a 10-kDa centrifugal spin filter (Millipore) and washed with 200 μL of 8 M urea three times and 200 μL of 50 mM ammonium bicarbonate twice via centrifugation at 14,000 × *g*. Next, tryptic digestion was performed by adding trypsin (Promega) at a ratio of 1:50 (enzyme/substrate, m/m) to 200 μL of 50 mM ammonium bicarbonate at 37 °C for 16 h. The peptides were recovered by transferring the filter to a new collection tube and centrifuging at 14,000 × *g*. The peptide yield was increased by washing the filter with 100 μL of 50 mM $NaHCO_3$ twice. The peptides were desalted using a StageTip.

MS experiments were performed on a nanoscale UHPLC system (EASY-nLC1000 from Proxeon Biosystems) connected to an Orbitrap Q-Exactive equipped with a nano-electrospray source (Thermo Fisher). The peptides were dissolved in 0.1% FA with 5% CH_3CN and separated on an RP-HPLC analytical column (75 μm × 15 cm) packed with 2-m C18 beads (Thermo Fisher) using a 2-h gradient from 5 to 40% acetonitrile in 0.5% formic acid at a flow rate of 250 nL/min. The spray voltage was set to 2.5 kV, and the temperature of the ion transfer capillary was 275 °C. A full MS/MS cycle consisted of one full MS scan (resolution at 70,000; automatic gain control [AGC] value, 1e6; maximum injection time, 50 ms) in the profile mode over a mass range of *m/z* 300 and 1,800, followed by fragmentation of the 10 most intense ions via high-energy collisional dissociation with normalized collision energy at 28% in the centroid mode (resolution, 17,500; AGC value, 1e5; maximum injection time, 100 ms). Moreover, the dynamic exclusion window was set to 40 s, and one microscan was acquired for each MS and MS/MS scan. Subsequently, the unassigned ions and those with a charge of 1+ and > 7+ were rejected for MS/MS, and a lock mass correction using a background ion (*m/z* 445.12003) was applied (33). The raw data were processed using Proteome Discoverer (PD, version 2.1), and the MS/MS spectra were used to search the reviewed UniProt human proteome database. All the searches were performed with a precursor mass tolerance of 7 ppm and a fragment mass tolerance of 20 millimass units, with oxidation (Met) (+15.9949 Da) and acetylation (protein N termini) (+42.0106 Da) as variable modifications, carbamidomethylation (+57.0215 Da) as the fixed modification, and allowance for two trypsin-missed degradations. Only the peptides of at least six amino acids were considered. The peptide and protein

identifications were filtered by PD to control the false discovery rate at <1%. At least one unique peptide was required for protein identification.

Isolation of Membrane-Associated Proteins. The isolation of membrane-associated proteins was performed using the Mem-PERPlus Membrane Protein Extraction Kit (Invitrogen) (28). In summary, cells were harvested from suspension cell cultures by centrifugation at 300 × *g* for 5 min. The obtained cell pellets were washed with 3 mL of Cell Wash Solution and centrifuged at 300 × *g* for 5 min. After supernatants were removed, the cell pellets were resuspended with 1.5 mL of Cell Wash Solution, transferred to a new tube, and centrifuged at 300 × *g* for 5 min to discard the supernatants. The resultant cell pellets were mixed with 0.75 mL of permeabilization buffer to obtain a homogeneous cell suspension and incubated for 10 min at 4 °C. Next, the permeabilized cells were centrifuged at 16,000 × *g* for 15 min, and the resultant supernatants containing cytosolic proteins were removed and transferred to a new tube for detection. Next, the pellets were resuspended with 0.5 mL of solubilization buffer, and the mixtures were incubated at 4 °C with constant mixing for 30 min. The resultant solution in the tubes was centrifuged at 16,000 × *g* at 4 °C for 15 min. The supernatants containing the solubilized membrane and membrane-associated proteins were moved to a new tube for analysis; the proteins were subjected with sodium dodecyl sulfate polyacrylamide gel electrophoresis (SDS-PAGE) and detected with various antibodies during Western blotting.

HIV-1 Virion Enrichment Assay. The cell culture media containing HIV-1 particles were centrifuged at 1,200 × *g* for 5 min. The supernatants were passed through a 0.45-μm filter (Thermo Fisher) and layered on 20% sucrose for a 2-h ultracentrifugation at 25,000 × *g* at 4 °C. The virion pellets were subsequently isolated using anti-CD44 microbeads with a magnetic-based method according to the manufacturers' instructions (μMACS VitalVirus HIV Isolation Kit; Miltenyi Biotec). The purified virions were lysed with RIPA buffer (Thermo Fisher) and subjected to SDS-PAGE for Western blotting.

HIV-1 Attachment Assay. The attachment of the viral particles was assayed (34, 35). In summary, 3×10^5 TZM-bl cells or 2×10^5 stimulated $CD4^+$ T cells were spinoculated with HIV-1 at 1,200 × *g* at 25 °C for 2 h. Then, the infected cells were washed with cold media five times to remove the unbound viral particles. Next, the cells were lysed with 0.5% Triton X-100 to quantify the cell-associated p24gag using ELISA. Virion equivalents were determined by assuming an average of 1,500 p24gag molecules per HIV-1 particle, in other words, 15,800 viral particles per picogram of p24gag.

The BlaM-Vpr–Based Viral Entry Assay. HIV-1 particles incorporating a fusion protein between Vpr and BlaM reporter protein were produced by cotransfection of NL4-3-Luc-R^+-E^- with an expression vector encoding BlaM-Vpr. The viruses that were produced were quantified by p24 ELISA, and target cells were incubated with 100 ng of p24 viruses at 37 °C for 4 h to allow viral entry. After washing three times with Hank's balanced salt solution (HBSS) (Thermo Fisher), cells were resuspended and loaded with 1 μM CCF2-AM dye (Thermo Fisher), a fluorescent substrate for BlaM, in HBSS containing 1 mg/mL Pluronic F-127 surfact (Thermo Fisher) and 0.001% acetic acid for 1 h at room temperature and then washed twice with HBSS. The BlaM reaction, which corresponds to the cleavage of intracellular CCF2 dye by BlaM-Vpr, was developed for 14 h at room temperature in HBSS supplemented with 10% FBS. Cells were washed three times with PBS and fixed in a 1.2% solution of paraformaldehyde. The fluorescence was monitored at 520 nm and 447 nm by means of flow cytometry using SONY ID7000.

Western Blotting and Antibodies. Standard Western blotting was performed to detect cellular proteins using various antibodies, including monoclonal rabbit anti-NRP-1 (catalog no. ab81321, 1:1,000 dilution; Abcam), polyclonal goat anti-gp120 (catalog no. ARP-288, 1:20,000; NIH AIDS Reagent Program), rabbit anti-GAPDH (catalog no. PA1-987, 1:1,000; Thermo Fisher), mouse monoclonal anti-FLAG (catalog no. F1804, 1:1,000; Sigma), rabbit polyclonal anti-p24 (catalog no. ab63913, 1:1,000; Abcam), and mouse Igs-HRP (catalog no. 6789, 1:5,000; Abcam).

Microscopy. The cells were photographed using the Thermo Fisher EVOS FL Imaging System.

qPCR. Total RNA was extracted from the cells using TRIzol (Invitrogen). Then, the obtained RNA was dissolved in 100 μL of DPEC-H_2O, and 1 μg of the purified RNA was treated with DNase I (amplification grade, Invitrogen) for 10 to 15 min at room temperature. Next, the RNA was immediately primed with oligo-dT and reverse-transcribed using the SuperScript III Reverse Transcriptase (Invitrogen). Afterward, real-time PCR analysis was performed using the ΔΔCT method with various primer sets (*SI Appendix*, Table S2). Finally, the results were normalized to the amplification results of the internal control, GAPDH.

Statistical Analysis. Statistical analysis was performed using Prism 6.0 (GraphPad Software). Unpaired two-tailed Student's *t* tests were used for statistical comparison between groups, unless otherwise specifically mentioned. Each experiment was performed three times independently, and the data were presented as the mean ± SEM.

Data Availability. All study data are included in the article and/or *SI Appendix*.

ACKNOWLEDGMENTS. We thank all our laboratory members for contributing to this study. We also thank Shengjia Li for technical support. This study was supported by National Key R&D Program of China (Grant 2021YFC2301900) and National Natural Science Foundation of China Grant 82072284.

1. H. Koppensteiner, R. Brack-Werner, M. Schindler, Macrophages and their relevance in Human Immunodeficiency Virus Type I infection. *Retrovirology* **9**, 82 (2012).
2. W. R. Heath, F. R. Carbone, Dendritic cell subsets in primary and secondary T cell responses at body surfaces. *Nat. Immunol.* **10**, 1237–1244 (2009).
3. V. Piguet, R. M. Steinman, The interaction of HIV with dendritic cells: Outcomes and pathways. *Trends Immunol.* **28**, 503–510 (2007).
4. F. O. Martinez, A. Sica, A. Mantovani, M. Locati, Macrophage activation and polarization. *Front. Biosci.* **13**, 453–461 (2008).
5. K. Kedzierska, S. M. Crowe, The role of monocytes and macrophages in the pathogenesis of HIV-1 infection. *Curr. Med. Chem.* **9**, 1893–1903 (2002).
6. M. S. Meltzer, H. E. Gendelman, Mononuclear phagocytes as targets, tissue reservoirs, and immunoregulatory cells in human immunodeficiency virus disease. *Curr. Top. Microbiol. Immunol.* **181**, 239–263 (1992).
7. N. Laguette *et al.*, SAMHD1 is the dendritic- and myeloid-cell-specific HIV-1 restriction factor counteracted by Vpx. *Nature* **474**, 654–657 (2011).
8. K. Hrecka *et al.*, Vpx relieves inhibition of HIV-1 infection of macrophages mediated by the SAMHD1 protein. *Nature* **474**, 658–661 (2011).
9. D. Ghez *et al.*, Neuropilin-1 is involved in human T-cell lymphotropic virus type 1 entry. *J. Virol.* **80**, 6844–6854 (2006).
10. R. K. Lane *et al.*, Necroptosis-based CRISPR knockout screen reveals Neuropilin-1 as a critical host factor for early stages of murine cytomegalovirus infection. *Proc. Natl. Acad. Sci. U.S.A.* **117**, 20109–20116 (2020).
11. L. Cantuti-Castelvetri *et al.*, Neuropilin-1 facilitates SARS-CoV-2 cell entry and infectivity. *Science* **370**, 856–860 (2020).
12. J. L. Daly *et al.*, Neuropilin-1 is a host factor for SARS-CoV-2 infection. *Science* **370**, 861–865 (2020).
13. C. Liu *et al.*, Neuropilin-1 is a T cell memory checkpoint limiting long-term antitumor immunity. *Nat. Immunol.* **21**, 1010–1021 (2020).
14. B. Chaudhary, Y. S. Khaled, B. J. Ammori, E. Elkord, Neuropilin 1: Function and therapeutic potential in cancer. *Cancer Immunol. Immunother.* **63**, 81–99 (2014).
15. T. Kawasaki *et al.*, A requirement for neuropilin-1 in embryonic vessel formation. *Development* **126**, 4895–4902 (1999).
16. T. Kitsukawa *et al.*, Neuropilin-semaphorin III/D-mediated chemorepulsive signals play a crucial role in peripheral nerve projection in mice. *Neuron* **19**, 995–1005 (1997).
17. C. Gu *et al.*, Neuropilin-1 conveys semaphorin and VEGF signaling during neural and cardiovascular development. *Dev. Cell* **5**, 45–57 (2003).
18. S. Roy *et al.*, Multifaceted role of neuropilins in the immune system: Potential targets for immunotherapy. *Front. Immunol.* **8**, 1228 (2017).
19. A. L. Kolodkin *et al.*, Neuropilin is a semaphorin III receptor. *Cell* **90**, 753–762 (1997).
20. C. C. Lee, A. Kreusch, D. McMullan, K. Ng, G. Spraggon, Crystal structure of the human neuropilin-1 b1 domain. *Structure* **11**, 99–108 (2003).
21. C. W. Vander Kooi *et al.*, Structural basis for ligand and heparin binding to neuropilin B domains. *Proc. Natl. Acad. Sci. U.S.A.* **104**, 6152–6157 (2007).
22. B. A. Appleton *et al.*, Structural studies of neuropilin/antibody complexes provide insights into semaphorin and VEGF binding. *EMBO J.* **26**, 4902–4912 (2007).
23. M. W. Parker, P. Xu, X. Li, C. W. Vander Kooi, Structural basis for selective vascular endothelial growth factor-A (VEGF-A) binding to neuropilin-1. *J. Biol. Chem.* **287**, 11082–11089 (2012).
24. Y. C. Tsai *et al.*, Structural studies of neuropilin-2 reveal a zinc ion binding site remote from the vascular endothelial growth factor binding pocket. *FEBS J.* **283**, 1921–1934 (2016).
25. F. Nakamura, M. Tanaka, T. Takahashi, R. G. Kalb, S. M. Strittmatter, Neuropilin-1 extracellular domains mediate semaphorin D/III-induced growth cone collapse. *Neuron* **21**, 1093–1100 (1998).

26. T. Yelland, S. Djordjevic, Crystal structure of the neuropilin-1 MAM domain: Completing the neuropilin-1 ectodomain picture. *Structure* **24**, 2008–2015 (2016).
27. J. J. Monsuez *et al.*, HIV-associated vascular diseases: Structural and functional changes, clinical implications. *Int. J. Cardiol.* **133**, 293–306 (2009).
28. G. Liang *et al.*, Membrane metalloprotease TRABD2A restricts HIV-1 progeny production in resting $CD4^+$ T cells by degrading viral Gag polyprotein. *Nat. Immunol.* **20**, 711–723 (2019).
29. L. Zhao *et al.*, Vpr counteracts the restriction of LAPTM5 to promote HIV-1 infection in macrophages. *Nat. Commun.* **12**, 3691 (2021).
30. R. I. Connor, B. K. Chen, S. Choe, N. R. Landau, Vpr is required for efficient replication of human immunodeficiency virus type-1 in mononuclear phagocytes. *Virology* **206**, 935–944 (1995).
31. T. Gramberg *et al.*, Restriction of diverse retroviruses by SAMHD1. *Retrovirology* **10**, 26 (2013).
32. M. Llano *et al.*, An essential role for LEDGF/p75 in HIV integration. *Science* **314**, 461–464 (2006).
33. J. R. Wiśniewski, A. Zougman, N. Nagaraj, M. Mann, Universal sample preparation method for proteome analysis. *Nat. Methods* **6**, 359–362 (2009).
34. U. O'Doherty, W. J. Swiggard, M. H. Malim, Human immunodeficiency virus type 1 spinoculation enhances infection through virus binding. *J. Virol.* **74**, 10074–10080 (2000).
35. W. J. Swiggard *et al.*, Human immunodeficiency virus type 1 can establish latent infection in resting CD4+ T cells in the absence of activating stimuli. *J. Virol.* **79**, 14179–14188 (2005).